Journal of Constructional Steel Research 98 (2014) 178–187

Contents lists available at ScienceDirect

Journal of Constructional Steel Research

Hybrid damping systems in offshore jacket platforms with float-over deck

Ali Jafarabad [a,*], Majid Kashani [b], Mohammad Reza Adl Parvar [a], Ali Akbar Golafshani [b]

[a] Civil Engineering Department, University of Qom, Qom, P.O. Box 3716146611, Iran
[b] Civil Engineering Department, Sharif University of Technology, Tehran, P.O. Box 11155-9313, Iran

ARTICLE INFO

Article history:
Received 26 July 2012
Accepted 12 February 2014
Available online 22 April 2014

Keywords:
Offshore jacket platform
Wave-induced fatigue damage
Seismic load
Friction damper
Tuned mass damper
Hybrid damping system

ABSTRACT

Employing dampers to control wave-induced and seismic vibrations of offshore jacket platforms is an attractive method in order to mitigate fatigue and seismic damage. However, adjustable parameters of a damper are designed by considering only one type of environmental loads; either normal-condition load or extreme-condition load. So, it is important to investigate effectiveness of damping system, for both of two main categories of environmental loads. Also it is ideal for the system to have an acceptable performance in both normal and extreme conditions. The idea investigated in the current study is to use a friction damper device (FDD) and a tuned mass damper (TMD) simultaneously in offshore jacket platforms with float-over deck to control both fatigue damage as well as seismic vibration. To develop the idea, adjustable parameters of FDD and TMD have been adjusted for wave loading. Afterward, they are combined with those designed for earthquake, so the hybrid damping system (HDS) is introduced. By introducing HDS, it is intended to make damping system have a high seismic performance while being effective in fatigue damage mitigation. Moreover, HDS can have different combinations. So, certain variants of HDS are determined which have much higher performance than the other variants.

1. Introduction

Periodical inspections have demonstrated that offshore platforms in the Persian Gulf are highly vulnerable to fatigue damage during their operational life. Such investigations provide evidence that tubular members can experience significant damage including loss of cross sectional area, indicating that the fatigue damage should be considered more seriously in order to extend the operational life of offshore platforms. Nowadays, one third of the existing offshore platforms require life extension [1] and life extension process requires structural rehabilitation. Many researchers have put their focus on various methods for rehabilitating damaged or extra-loaded platforms and fatigue damage mitigation of offshore structures. Conventional rehabilitation methods can impose excessive cost of underwater welding and fabrication included in those processes, so a novel technology is proposed by researchers. This technology is to equip existing or even new offshore platforms with vibration control devices. Vibration control of offshore jacket platforms is very attractive because in general, reduction of the dynamic stress amplitude of an offshore structure by 15% can extend the service life over two times, and can result in decreasing the expenditure on the maintenance and inspection of the structure [2].

On the other hand, offshore platforms are of the economic life lines of oil-rich countries, so it is a serious problem on how to guarantee their immediate occupancy after earthquakes. Again, one proposed method to solve the problem is to employ vibration control devices. Some researchers have worked on this topic and have found it effective to use those devices to control seismic vibrations.

Among those who have studied vibration control of offshore platforms are Vincenzo and Roger [3], Ou et al. [4], Li et al. [5], Wang [6], Mahadik and Jangid [7], Zhou and Zhao [8], Patil and Jangid [9], Lee et al. [10], Ou et al. [2], Jin et al. [11], Ma et al. [12], Xu et al. [13], Yue et al. [14], Taflanidis et al. [15] and Kim [16]. All of them have found it effective to use control mechanisms for mitigation of vibrations induced by different environmental loads.

Recently, in some studies [17,18] adjustable parameters of one type of FDD have been optimized for realistic jacket platforms for wave-induced hydrodynamic loads. Moreover, Gholizad [19] has optimized TMD for use against wave-induced fatigue damage. Those works play a key role in the current study, since they are among several sources approached in order to obtain comprehensive data on the subject.

Offshore jacket platforms, located at severe environmental conditions, are generally subjected to two main categories of environmental loading, i.e. normal-condition loads such as wave-induced hydrodynamic force and extreme-condition loads like seismic excitation. The former external force has a significant contribution to fatigue damage which causes the excessive cost of rehabilitation and the latter one

* Corresponding author. Tel.: +98 912 2716259.
E-mail addresses: a.jafarabad@stu.qom.ac.ir, m_bank_65@yahoo.com (A. Jafarabad).

http://dx.doi.org/10.1016/j.jcsr.2014.02.004
0143-974X/

can endanger the serviceability of offshore jacket platforms which are of the economic life lines of oil-rich countries.

Employing novel devices to control the wave-induced and seismic vibrations is an attractive method in order to mitigate fatigue damage and to guarantee immediate occupancy of offshore platforms after earthquakes. But, adjustable parameters of a vibration control system for offshore platforms are generally designed by considering only one type of environmental loading; either normal-condition load or extreme-condition load. So, it is important to investigate the effectiveness of vibration control system, for both of the two main categories of environmental loads.

The overall objective of this study is to investigate the idea of combining dampers with different designs to control both of two main categories of environmental loads exerted upon offshore platforms which are classified into normal-condition loads and extreme-condition loads. It is to be determined which combination of dampers is the most effective. So far, some other aspects of the idea of employing HDS in offshore jacket platforms have been discussed elsewhere in some papers [20,21].

2. Class of offshore platform under study

The jacket, the piles, and the deck are the main structural components of the offshore jacket platform. For topside installation, all deck facilities are fabricated into modules and then transported by barge and set on the platform by a derrick. Float-over decks are a development which enables the prefabrication of the complete topsides, so that it may be transported by barge and set as a complete unit on the preinstalled jacket [22]. With making use of float-over decks, some limitations are imposed over the characteristics of the platform. Float-over deck requires omission of bracings in one direction at the water surface level, in order to allow the barge to move between legs of the jacket and install the deck, so the stiffness of the platform at this level is very low compared to other levels.

Limitations of high flexibility of the upper elevation in one direction can be counteracted by making use of auxiliary vibration control devices.

In the current study, two realistic float-over-deck offshore jacket platforms shown in Fig. 1 are examined; "North Rankin B" (NRB) is a platform installed on Western Australia offshore oil fields with a height of 125 m and "Foroozan" (FRZ) is a six leg platform located in waters of the Persian Gulf with a height of 95 m. As their topsides have been installed with float-over technique, the bracings have been omitted in one direction at the water surface level. As a consequence, making use of auxiliary vibration control devices is a novel suggestion to counteract the effects of high flexibility at the upper levels of the jacket.

An idealized three-degree-of-freedom (3DOF) system (Fig. 2) is considered as the structural model for each platform. The values of lumped mass and pre-yielding stiffness have been determined by Golafshani and Gholizad [17] in a way that the overall model would have the same natural period and kinetic energy for each mode of vibration as the real overall platform. Some detailed descriptions of structural models, such as pre-yielding stiffness and lumped mass values, are listed in Table 1. In this table the m_1, m_2 and m_3 parameters are respectively the lumped mass of the first, second and third stories of the idealized 3DOF model of the platforms and the k_1, k_2 and k_3 parameters are respectively the stiffness of the first, second and third stories of the model. For each platform a proportional damping matrix is determined by considering the damping ratio for the first three modes of vibration to be 0.05, 0.03 and 0.02 [17].

3. Damping systems

3.1. FDD

FDD is a novel friction damper which can have many various models and configurations. It has been innovated by Mualla [23,24]. One simple configuration of FDD is shown in Fig. 3 This new damper device is based on friction between pad disks and steel plates. Simplicity of concept and

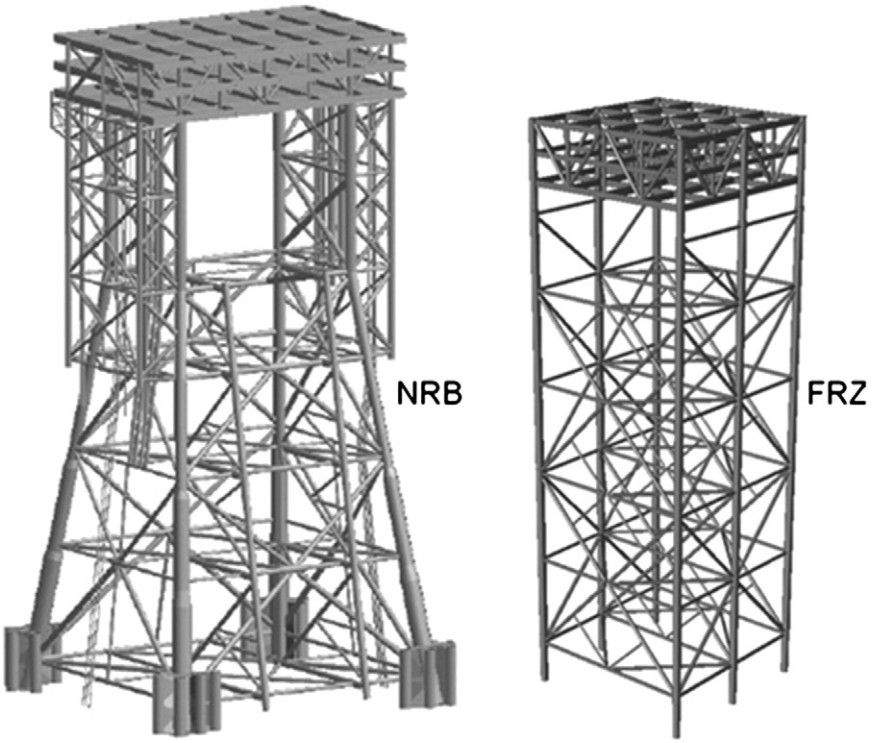

Fig. 1. Case study platforms [17].

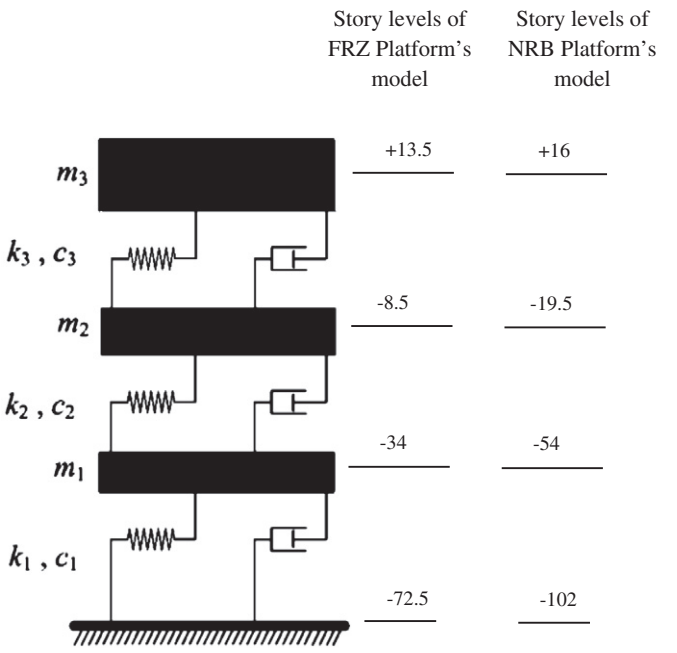

Fig. 2. Modeling of the platforms by idealized three-degree-of-freedom (3DOF) system.

design allows this device to be constructed for projects with space limitation and high force level.

Mualla and Belev [24] have proposed an analytical model for their innovated FDD which yields to an idealized hysteretic behavior, shown in Fig. 4, in which there are two design parameters of k_{FDD} and D_{FDD} determining the general shape of the hysteresis loop. As can be inferred in Fig. 4, k_{FDD} is the brace stiffness of FDD and D_{FDD} is the sliding (slip-initiation) deformation. Consequently, the magnitude of FDD restoring force has a maximum equal to k_{FDD} D_{FDD}, i.e. the slip force. Behavior of FDD has two stages, i.e. stick phase and slip phase. Stick phase is when the deformation has not reached to the value of slip-initiation deformation and slip phase begins when the deformation exceeds that value.

3.2. TMD

Shown schematically in Fig. 3, TMD consists of a mass-spring-dashpot system anchored or attached to the main structure. This typical TMD works by absorbing the resonant portions of the frequency band of external excitation. Therefore, by transferring some of input energy to TMD, energy dissipation demand on the primary structural members will be reduced [25].

A typical TMD has three design parameters, i.e. mass, damping and stiffness, needed for the mathematical modeling. Those parameters are adjusted based on the fundamental frequency of the structure and also on the dominant frequency of external excitation in order to reduce vibrations induced by resonant phenomenon. Conventionally, the value of TMD mass is assumed based on the practical issues and the two other parameters are designed to achieve an acceptable performance.

3.3. HDS

As schematically shown in Fig. 3, FDD and TMD are simultaneously used for the structure to make a hybrid damping system or HDS. This hybrid system of dampers can have different variants on the basis of design of FDD and TMD which can be made against different loads such as earthquake and wave-induced fatigue. HDS is a combination of FDD and TMD each of which can have two designs, either seismic design or fatigue design. Consequently, HDS can have four possible variants as listed in Table 2. Summarized in Table 2 are the symbols used to illustrate HDS variants. Each symbol represents one particular structural system. For convenient referring and comparison, two symbols are used, the short symbol and the long symbol. Performance evaluation of different systems will be demonstrated in Section 6.3 with the vast usage of defined system identifiers.

3.4. Placement of FDD, TMD and HDS

In Section 2 it was mentioned that the float-over installation technique requires omission of bracings in one direction at the water surface level, so a good space there exists in this elevation for installation of FDD to rehabilitate the jacket platform. So, FDD is placed in the elevation at which the bracings are omitted due to float-over installation, where device is out of water. Location of FDD with respect to the idealized three degree of freedom system, discussed in Section 2, is demonstrated in Fig. 5, in which FDD, having a stiffness of k_{FDD}, is placed at the 3rd story of the structural model.

In order to install TMD, a space on the topside deck is required. TMD is located at the topside of jackets where it is above water surface elevation and more effective in the first mode of vibration [20].

4. Adjustment methodologies of damping systems

Golafshani and Gholizad [17] have optimized adjustable parameters of FDD for FRZ and NRB platforms. Their final optimization results are employed in the current study.

Innovative approaches for adjusting of friction damper for seismic load on the basis of performance-based design have been proposed by some authors such as Kim and Seo [26] and Kim and Choi [27]. With making use of this methodology, the target equivalent viscous damping ratio (β_d) and consequently optimal values of brace stiffness and slip-initiation deformation of FDD can be estimated. In this study, the adjustable parameters of FDD are calculated for a β_d of 20% for NRB platform and 18% for FRZ platform.

Based on the results of previous works [19,18] adjustment of TMD for wave-induced fatigue damage is conducted by tuning its frequency to a value between the central frequency of center-of-damage sea-state, which is equal to 0.974, and the fundamental frequency of the structure. The final results for the adjusted frequency of TMD for the NRB and FRZ platforms will be equal to 0.969 (rad/s) and 1.489 (rad/s), respectively. The complete explanation of the computations of these results was presented in the above references.

Determination of the optimal parameters of TMD subjected to different types of excitations has been investigated by several researchers. In the present study, adjustable parameters of TMD for earthquake are determined by the procedure proposed by Sadek et al. [28] that is suitable for multi-degree-of-freedom systems in which the structure has structural viscous damping. Sadek et al. [28] have defined mass ratio μ as

Table 1
Dynamic characteristics of case study platforms [17].

Platform	Fundamental frequency of the overall platform (rad/s)	k_1 (MN/m or ton/cm[a])	k_2 (MN/m or ton/cm[a])	k_3 (MN/m or ton/cm[a])	m_1 (ton[a])	m_2 (ton[a])	m_3 (ton[a])
NRB	1.023	400	430	39	9000	11,000	31,000
FRZ	2.095	335	365	32	1450	2050	6100

[a] ton: 1000 kg.

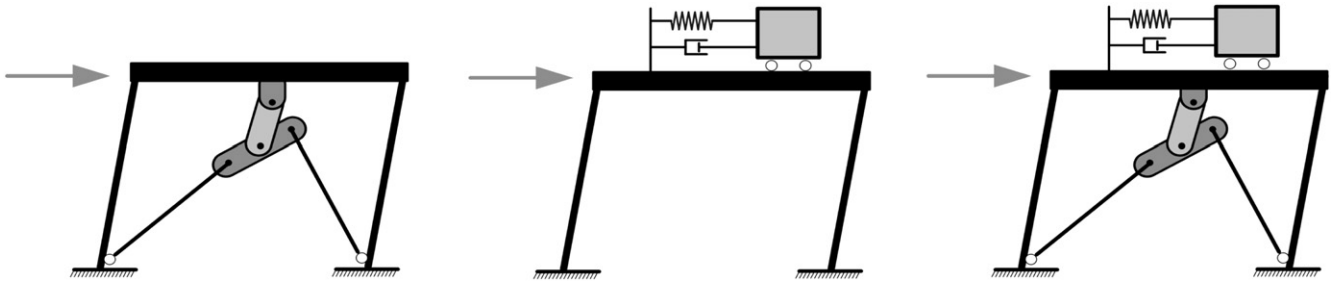

Fig. 3. Schematic illustration of FDD, TMD and HDS mounted on a frame structure [20].

the ratio of the TMD mass to the generalized mass for the fundamental mode for a unit modal participation factor (*MPF*), in the following expressions.

$$\mu = \frac{m_{TMD}}{\phi_1^T[M]\phi_1} \quad \text{for} \quad MPF_1 = \frac{\phi_1^T[M]\{1\}}{\phi_1^T[M]\phi_1} = 1 \tag{1}$$

m_{TMD}, $[M]$, $\{1\}$ and ϕ_1 are, respectively, TMD mass, structure mass matrix, unit vector and the fundamental mode shape normalized to have a unit participation factor. Adjustable parameter, the tuning ratio of the TMD (f), has been given by

$$f = \frac{\omega_{TMD}}{\omega_1} \tag{2}$$

where ω_{TMD} and ω_1 are the frequency of TMD and the fundamental frequency of the structure, respectively. Finally, the optimal TMD tuning ratio (f) has been proposed as

$$f = \frac{1}{1+\mu\Phi}\left(1-\beta\sqrt{\frac{\mu\Phi}{1+\mu\Phi}}\right) \tag{3}$$

where β is the structure damping ratio for the first mode of vibration (0.05) and Φ is the amplitude of the first mode for a unit modal participation factor computed at the location of the TMD, i.e. top of jacket. Assumed value for mass ratio μ is equal to that of TMD adjusted for wave loadings which is taken as 0.045. Computed optimal parameter of f for both platforms will be equal to 0.944. The final results for the adjusted frequency of TMD for the NRB and FRZ platforms will be equal to the 0.965 (rad/s) and 1.978 (rad/s), respectively, which are used in numerical simulations.

5. Simulation and modeling

5.1. Assumptions

Some of the main assumptions in the numerical simulations are summarized here. First of all, structural models have a nonlinear or hysteretic behavior. Fluid–structure interaction (FSI) is modeled in the case of seismic loading in order to evaluate seismic performance of HDS variants. Also only the most probable sea state, i.e. center-of-damage sea state, that was used by Golafshani and Gholizad [18] and was based on a sea scatter diagram of North Sea, is considered in spectral analyses for evaluation of fatigue performance of HDS variants.

The effect of the soil–structure interaction (SSI) and soil–pile interaction (SPI) can be described as follows. As it was explained in the second section, the dynamic characteristics of the structural model of each platform were determined in such a way that the model would have the same natural period and kinetic energy for each mode of vibration as the real platform. Since the effect of the SSI and SPI has been considered in the determination of the natural period of real platform, then it means that the general effect of the SSI and SPI has been considered in the characteristics of the structural model of each platform. The other secondary consequences of SSI and SPI such as the deduction of soil's stiffness in the severe earthquakes are ignored in this paper.

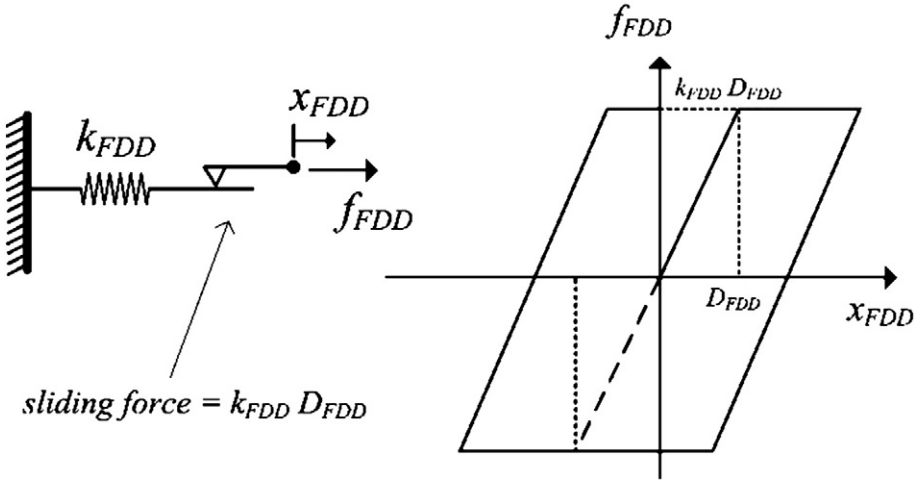

Fig. 4. Force-deformation hysteretic diagram for FDD after Mualla and Belev [24].

Table 2
HDS variants.

Short symbol	Long symbol	Description
HDS1	FDD for fatigue + TMD for fatigue	Structure equipped with HDS in which FDD is adjusted for fatigue and TMD is adjusted for fatigue
HDS2	FDD for quake + TMD for quake	Structure equipped with HDS in which FDD is adjusted for quake and TMD is adjusted for quake
HDS3	FDD for fatigue + TMD for quake	Structure equipped with HDS in which FDD is adjusted for fatigue and TMD is adjusted for quake
HDS4	FDD for quake + TMD for fatigue	Structure equipped with HDS in which FDD is adjusted for quake and TMD is adjusted for fatigue

5.2. Mathematical modeling

The equations of dynamic motion for an offshore platform idealized as 3DOF system with hysteretic behavior equipped with HDS in the 3rd story and subjected to external load of wave or earthquake can be written by coupled equations as shown below.

$$[M]\{x\}+[C]\{\dot{x}\}+\{f_s\}+\begin{Bmatrix}0\\-f_{FDD}\\f_{FDD}\end{Bmatrix}+\begin{Bmatrix}0\\0\\c_{TMD}\dot{z}+k_{TMD}z\end{Bmatrix}=\{f_{external}\} \tag{4}$$

$$m_{TMD}z+c_{TMD}\dot{z}+k_{TMD}z=-m_{TMD}x_{top\,total} \tag{5}$$

$$\{f_{external}\}=\begin{cases}\{f_{Morison}\}\text{ if wave}\\-[M]\{1\}x_g+\{f_{FSI}\}\text{ if quake}\end{cases} \tag{6}$$

Equations of structure and TMD must be simultaneously solved because they are coupled with each other. $\{x\}$, $[M]$, $[C]$, $\{f_s\}$, f_{FDD}, $\{f_{external}\}$, $\{f_{Morison}\}$, $\{1\}$, x_g, $\{f_{FSI}\}$, m_{TMD}, c_{TMD}, k_{TMD}, z and $x_{top\,total}$ are, respectively, the displacement vector, mass matrix, proportional damping matrix, stiffness restoring force vector, control force vector due to FDD, external load vector due to earthquake or wave, Morison wave load vector (refer to Section 5.3), unit vector, ground acceleration, force vector due to FSI, TMD mass, TMD damping, TMD stiffness, displacement of TMD relative to the top of jacket and total acceleration at the top of jacket.

Since the structure is assumed to have a nonlinear or hysteretic behavior, the stiffness force vector $\{f_s\}$ can be written by hysteresis models. Also, the force vector due to FDD $\{f_{FDD}\}$ can be simulated by hysteresis models. For modeling of $\{f_s\}$ and f_{FDD}, one notation of the Bouc–Wen model [29] used by Yang et al. [30] is adopted. Based on the Bouc–Wen model, the hysteretic force of FDD installed in the 3rd story, can be expressed as

$$f_{FDD}=\alpha_{FDD}k_{FDD}x_{FDD}+(1-\alpha_{FDD})k_{FDD}D_{FDD}v_{FDD} \tag{7}$$

in which α_{FDD} is the ratio of post-slip to pre-slip brace stiffness of FDD, x_{FDD} is the drift of the 3rd story, k_{FDD} is brace stiffness of FDD installed in the 3rd story, D_{FDD} is slip-initiation deformation of FDD and v_{FDD} is a non-dimensional variable introduced to describe the hysteresis component of the deformation, with the limitation of $|v_{FDD}|\le 1$, where

$$\dot{v}_{FDD}=D_{FDD}^{-1}\left(A_{FDD}\dot{x}_{FDD}-\beta_{FDD}|\dot{x}_{FDD}||v_{FDD}|^{n_{FDD}-1}v_{FDD}-\gamma_{FDD}\dot{x}_{FDD}|v_{FDD}|^{n_{FDD}}\right) \tag{8}$$

Parameters A_{FDD}, β_{FDD} and γ_{FDD} govern the scale and general shape of the hysteresis loop and n_{FDD} determines the smoothness of the force-deformation curve. To model a hysteresis loop that is appropriate for the FDD, parameters of Bouc–Wen model are considered as

$$\alpha_{FDD}=0.0,\quad A_{FDD}=1.0,\quad \beta_{FDD}=0.5,\quad \gamma_{FDD}=0.5,\quad \text{and}\quad n_{FDD}=95. \tag{9}$$

Methodology of simulation of $\{f_s\}$ by the Bouc–Wen model is similar to that of f_{FDD}. Parameters of Bouc–Wen model for $\{f_s\}$ are considered for all the three stories as

$$\alpha_s=0.1,\quad A_s=1.0,\quad \beta_s=0.5,\quad \gamma_s=0.5,\quad \text{and}\quad n_s=95 \tag{10}$$

The force vector $\{f_{FSI}\}$ is written as [31,16]

$$\{f_{FSI}\}=\rho(k_m-1)[V](\{\ddot{u}\}-\{\ddot{x}_{total}\})+\rho[V]\{\dot{u}\}+\rho k_d[A]\times\{|\dot{u}-\dot{x}_{total}|(\dot{u}-\dot{x}_{total})\} \tag{11}$$

$$\{\ddot{x}_{total}\}=\{\ddot{x}\}+\{1\}\ddot{x}_g\quad,\quad \{x_{total}\}=\{x\}+\{1\}x_g \tag{12}$$

Where ρ, k_m, k_d, $[V]$, $[A]$ and $\{u\}$ are the sea water density, inertia coefficient taken constant in depth as 2.0, drag coefficient taken constant in depth as 0.7, body volume matrix, projected area matrix and water particle horizontal motion vector, respectively. When the only load considered is due to ground motion, the water particle motion is neglected. In this case, water particle velocity vector and water particle acceleration vector would be equal to zero, and the force vector due to FSI can be written in the following form.

$$\{f_{FSI}\}=\rho(k_m-1)[V](-\{x_{total}\})+\rho k_d[A]\{|\dot{x}_{total}|(-\dot{x}_{total})\} \tag{13}$$

It is possible to use added mass concept and change the formulation of equations or even linearize the drag term, but in our numerical simulations, formulation of FSI force and its nonlinearity is preserved.

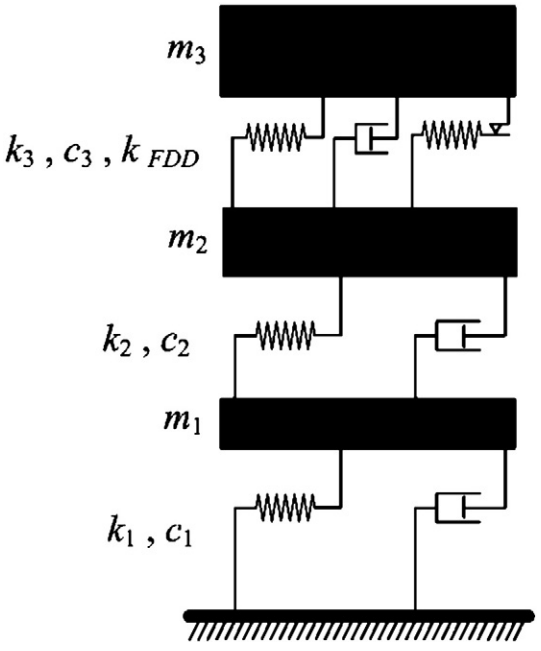

Fig. 5. Location of FDD in the idealized 3DOF system after Golafshani and Gholizad [17].

5.3. Selected technique for spectral analysis

This study is concerned with the spectral analysis of gravity waves generated by wind action. This type of surface water wave induces fatigue damage in offshore jacket platforms. Several approaches are

available in API RP2A-WSD [32] for determining structural response to sea-state loadings. Spectral analysis is recommended by API RP2A-WSD [32] to be used to properly account for the actual distribution of wave energy over the entire frequency range. The spectral approach has been subdivided by API RP2A-WSD [32] into three main methodologies as shown below, based upon the method used to develop transfer function.

1 Transfer functions developed using regular waves in the time domain.
2 Transfer functions developed using regular waves in the frequency domain.
3 Transfer functions developed using random waves in the time domain.

The first of the above-mentioned methodologies is employed in the current study. This methodology does not require any linearization, i.e. the drag term in the wave force expressed by Morison equation can be employed in its original non-linear form and also hysteretic behavior of both structural elements as well as FDD can be simulated. The objective is to compute variance of structural response with the aid of a transfer function from power spectral density function (PSDF) of wave height to PSDF of structural response. In this process a wave spectrum along with a wave theory is employed to create regular progressive waves. When each regular wave passes through the structure, with making use of nonlinear form of Morison equation, the force vector exerted upon the structure is determined. Structural analysis is conducted to compute structural response. Dividing the structural response by the wave height gives a point on the transfer function at the frequency of the regular wave. Moreover, the area under the PSDF of structural response will provide the variance value of response [33]. This characteristic is one important property of PSDF curve.

Characterization of the wave climate is carried out using PSDF of wave height or wave amplitude. In this study, to express unidirectional random wave loading, Pierson–Moskowitz wave height spectrum is employed [34,35] which is expressed as

$$S_{\zeta\zeta}(\omega) = \frac{124.37H_s^2}{T_z^4}\omega^{-5}\exp\left(\frac{-497.5}{T_z^4}\omega^{-5}\right) \tag{14}$$

in which H_s and T_z are significant wave height and wave zero up crossing period, respectively. H_s and T_z are adopted for the center-of-damage sea-state used by Golafshani and Gholizad [18].

Le Mehaute [36] provided a chart detailing applicability of various wave theories using wave steepness versus depth parameter in his description. In the current study, with making use of the linear wave theory originally developed by Airy [37], water surface profile is determined. Water surface elevation profile η can be written in the following form where k, ω, λ, T and g are the wave number, the wave frequency, the wave length, the wave period and acceleration due to gravity, respectively 37,34.

$$\eta(x,t) = a\sin(kx-\omega t) \tag{15}$$

$$k = \frac{2\pi}{\lambda} = \frac{\omega^2}{g} = \frac{4\pi^2}{gT^2} \tag{16}$$

The amplitude a of the water surface profile for a regular wave can be determined based on the frequency difference $\Delta\omega$ corresponding to that of a regular wave and the area under the wave spectrum, as expressed in the following equation [38,39].

$$a = \sqrt{2S_{\zeta\zeta}(\omega)\Delta\omega} \tag{17}$$

The next step is to compute the velocity and acceleration of water particles which are dependent upon the depth of water. The horizontal component of velocity and acceleration of water particles is expressed in the following mathematical formulas [37].

$$\dot{u}(x,y,t) = a\omega\frac{\cosh(k(y+d))}{\sinh(kd)}\sin(kx-\omega t) \tag{18}$$

$$u(x,y,t) = -a\omega^2\frac{\cosh(k(y+d))}{\sinh(kd)}\cos(kx-\omega t) \tag{19}$$

Making use of horizontal component of velocity and acceleration of water particles, we can employ Morison equation to compute the force vector exerted upon tubular members of jacket platforms for each regular wave [40]. So, the force vector becomes [31,16]

$$\{f_{Morison}\} = \rho(k_m-1)[V](\{\ddot{u}\}-\{\ddot{x}\}) + \rho[V]\{\dot{u}\} + \rho k_d[A]\{|\dot{u}-\dot{x}|(\dot{u}-\dot{x})\} \tag{20}$$

in which u and x are displacements of water particles and structural elements, respectively. In this study, the nonlinearity of Morison equation is taken into account.

After generating the force vector due to regular waves, dynamic analysis of each offshore platform under each regular wave force vector is conducted in order to obtain structural response. The analysis procedure must eliminate transient effects by achieving steady state conditions. So, a sufficient number of time steps in the wave cycle at which structural response is computed should be selected to determine the maximum structural response [32]. Dividing the maximum structural response in the steady state condition by the wave height gives a point on the transfer function at the frequency of the regular wave. After computing the enough number of points on the transfer function, PSDF of the platform response can be obtained as

$$S_{rr}(\omega) = |H_{r\zeta}(\omega)|^2 S_{\zeta\zeta}(\omega) \tag{21}$$

in which S_{rr}, $H_{r\zeta}$ and $S_{\zeta\zeta}$ are PSDF of structural response, transfer function and PSDF of wave height, respectively. So, PSDF of structural response is computed such as those shown in Fig. 6. It should be remembered that the center-of-damage sea state has been assumed for the computation of the transfer function and for each platform analysis. In the center-of-damage sea state, which is based on a sea scatter diagram of North Sea, the quantities of significant wave height (H_s) and wave zero up crossing period (T_z) are 1.88 (m) and 4.88 (s) respectively. Since the central frequency of wave spectrum and fundamental frequency of NRB platform are very close to each other, only one peak there exists in its PSDF of top displacement. In the PSDF of top displacement of the FRZ platform, the first peak is related to the central frequency of wave spectrum and the second one is because of the fundamental frequency of FRZ platform.

5.4. Record selection

For designing fixed offshore platforms against the earthquake load, API RP2A-WSD [32] recommends where the time history method is used, the design response should be calculated as the average of the peak values for each of the time histories considered. Moreover, based on requirements of FEMA 356 [41], where seven or more time history data sets are employed, the average value of each response parameter shall be permitted to determine design acceptability. Consequently, the number of records in the present two-dimensional study is finally selected not fewer than seven time histories [20]. So, 20 time histories are employed for seismic analysis.

Listed in Table 3, a subset of the PEER NGA database [42] and PEER Strong Motion Database [43] is used from which it is tried to exclude recordings that were believed to be near-field ground motions. Recent experiences show that near-field earthquakes have high peak acceleration and high velocity pulse. As they do not behave like far-field earthquakes,

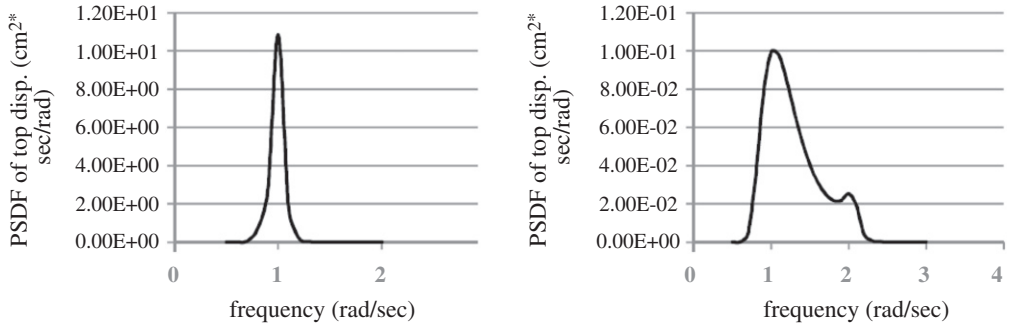

Fig. 6. PSDF of top displacement for NRB platform (left) and FRZ platform (right).

but like a shock, passive dampers may fail to dissipate input energy efficiently. As a result, mainly far-field records are taken into account by considering a Joyner–Boore distance of more than 40 km. Most of the used records have an average shear wave velocity, to a depth of 30 m, less than 180 m/s, considering a soft soil type for the sea bed. Moreover, some factors are used to scale records in order to ensure more compliance with API standard spectrum for soil type C and seismic zone 5 [32].

Verification of numerical simulations has been carried out by Kashani [44] and Kashani [20].

6. Results and discussion

6.1. Criteria and indices of fatigue performance

For later comparison of effectiveness of HDS variants in fatigue damage mitigation, two criteria and two performance indices are defined. The two criteria are top displacement and inter-story drift because of their direct correlation with accumulative fatigue damage [18]. The first performance index (J_1) is defined as the reduction percent of standard deviation of top displacement. The second performance index (J_2) is defined as the reduction percent of standard deviation of inter-story drift. Formulations of two fatigue performance indices are defined as below.

$$J_1 = 100\left(1-\frac{\sigma_{top,w}}{\sigma_{top,wo}}\right), J_2 = 100\left(1-\frac{\sigma_{drift,w}}{\sigma_{drift,wo}}\right) \quad (22)$$

in which $\sigma_{top,w}$ and $\sigma_{top,wo}$ are standard deviation of top displacement of structures with HDS and without HDS, respectively. $\sigma_{drift,w}$ and $\sigma_{drift,wo}$ are standard deviation of inter-story drift with HDS and without HDS, respectively. It should be noted that J_2 can be evaluated for each of stories of the platforms.

6.2. Criteria and indices of seismic performance

For later comparison of effectiveness of HDS variants in controlling seismic vibrations, two criteria, i.e. top displacement and inter-story drift, and two performance indices are defined. The average of the peak values for each of 20 records is determined for top displacement. Then, the third performance index (J_3) is defined to be equal to the reduction percent of that average value. Moreover, the average of the peak values for each of 20 records is determined for inter-story drift. The corresponding performance index (J_4) is defined by computing the reduction percent of that average value. Finally, the two seismic performance indices are defined as below.

$$J_3 = 100\left(1-\frac{P_{top,w}}{P_{top,wo}}\right), J_4 = 100\left(1-\frac{P_{drift,w}}{P_{drift,wo}}\right) \quad (23)$$

in which $P_{top,w}$ and $P_{top,wo}$ are average of the peak values of top displacement with HDS and without HDS, respectively. $P_{drift,w}$ and $P_{drift,wo}$ are average of the peak values of inter-story drift with HDS and without HDS, respectively. It should be noted that J_4 can be evaluated for each of stories of the platforms.

6.3. Performance evaluation

This section summarizes the main numerical results related to performance evaluation of four variants of HDS. For NRB platform, performance indices of all variants of HDS are listed in Table 4. J_2 and J_4, associated to inter-story drift, are presented for each of three stories of NRB platform. Fig. 7 presents the corresponding illustration. The radial axis in Fig. 7 shows the quantity of performance indices in logarithmic scale. Performance indices from J_1 to J_4 are organized in a counter clock wise order around the center point. For FRZ platform, performance indices are listed in Table 5 and the corresponding illustration is presented by Fig. 8.

According to Figs. 7 and 8, all the HDS variants have a similar effectiveness in J_1 and J_2. This fact makes it unnecessary to give different weights to fatigue performance indices (J_1 and J_2) and seismic performance indices (J_3 and J_4) and consequently simplifies the comparison. Since HDS variants have nearly the same values of J_1 and J_2, so the variant having higher values of J_3 and J_4 is the best one which is capable of controlling both fatigue damage as well as seismic vibrations. It is inferred in Figs. 7 and 8 that HDS4 and HDS2 are the best mechanisms for both NRB and FRZ platforms. As a consequence, by combining FDD designed for seismic load and TMD adjusted for wave-induced fatigue or seismic load, the resulted HDS would have the best total performance as compared to other variants of HDS. By employing HDS4 or HDS2 we can achieve the overall objective of this research: to control both fatigue damage as well as seismic vibrations.

Table 3
Selected records [20].

No	Record/component in the PEER	No	Record/component in the PEER	No	Record/component in the PEER	No	Record/component in the PEER
1	CHICHI06/CHY107-N	6	KOCAELI/ATS000	11	LOMAP/MEN270	16	CHICHI/CHY004-W
2	CHICHI/ILA004-N	7	LOMAP/A02043	12	LOMAP/MEN360	17	DUZCE/ATS030
3	IMPVALL/A-E03140	8	LOMAP/A02133	13	LOMAP/TRI000	18	KOBE/NIS000
4	IMPVALL/A-E03230	9	LOMAP/LKS270	14	NORTHR/WAT180	19	KOBE/NIS090
5	IMPVALL/H-E03230	10	LOMAP/LKS360	15	CHICHI/CHY004-N	20	KOBE/SHI000

Table 4
Performance indices of HDS variants (%), NRB platform.

System	J_1	J_2: 1st story	J_2: 2nd story	J_2: 3rd story	J_3	J_4: 1st story	J_4: 2nd story	J_4: 3rd story
HDS1: FDD for fatigue + TMD for fatigue	72.59	12.62	13.53	93.29	5.40	1.65	1.94	5.50
HDS2: FDD for quake + TMD for quake	72.58	11.87	12.76	93.50	16.86	14.09	13.18	19.95
HDS3: FDD for fatigue + TMD for quake	72.34	11.87	12.76	93.26	3.41	1.56	1.71	3.89
HDS4: FDD for quake + TMD for fatigue	72.93	12.61	13.51	93.66	16.66	14.40	13.66	19.96

One important point inferred from Figs. 7 and 8 is that fatigue performance indices (J_1 and J_2) have a much less sensitivity to design of dampers in comparison with seismic performance indices (J_3 and J_4). This fact is justified by investigating the spectrum of the two external loads in the frequency domain. The wave-induced load has an extremely simple PSDF which has only one peak and the range of effective frequencies is very limited (Eq. (14)). But either the Fourier amplitude or the acceleration spectrum of each of the earthquake records when plotted against frequency values is very complicated and has many fluctuations and peaks.

For seismic performance indices (J_3 and J_4), the HDS2 and HDS4 are more effective than HDS1 and HDS3. In HDS2 and HDS4, FDD is adjusted for seismic load, and in HDS1 and HDS3, FDD is adjusted for wave-induced load. Consequently, it is deduced that FDD seems to have much more influence on the effectiveness of HDS rather than TMD.

According to Tables 4 and 5, J_2 and J_4 for the first and second stories are generally much lower than those for third story, because, as can be seen in Table 1, the pre-yielding stiffness of the first and second stories is nearly ten times larger than that of the third story.

Fatigue performance indices (J_1 and J_2) are much larger for NRB platform than FRZ platform as demonstrated in Tables 4 and 5. But for seismic performance indices (J_3 and J_4), there is no general trend when comparing the two platforms. NRB platform has a larger value of fundamental period and its period is very close to the central frequency of the wave spectrum, so it is reasonable that HDS variants should have a higher fatigue performance indices (J_1 and J_2) for NRB platform as compared to FRZ platform.

7. Conclusions and recommendations

Analytical studies were undertaken to investigate the idea of using HDS variants in offshore jacket platforms in order to control both seismic vibration and fatigue damage. The main conclusions of the study are presented herein.

1 The idea of using HDS in offshore jacket platforms with float-over deck is quite effective in controlling both seismic vibration as well as fatigue damage.

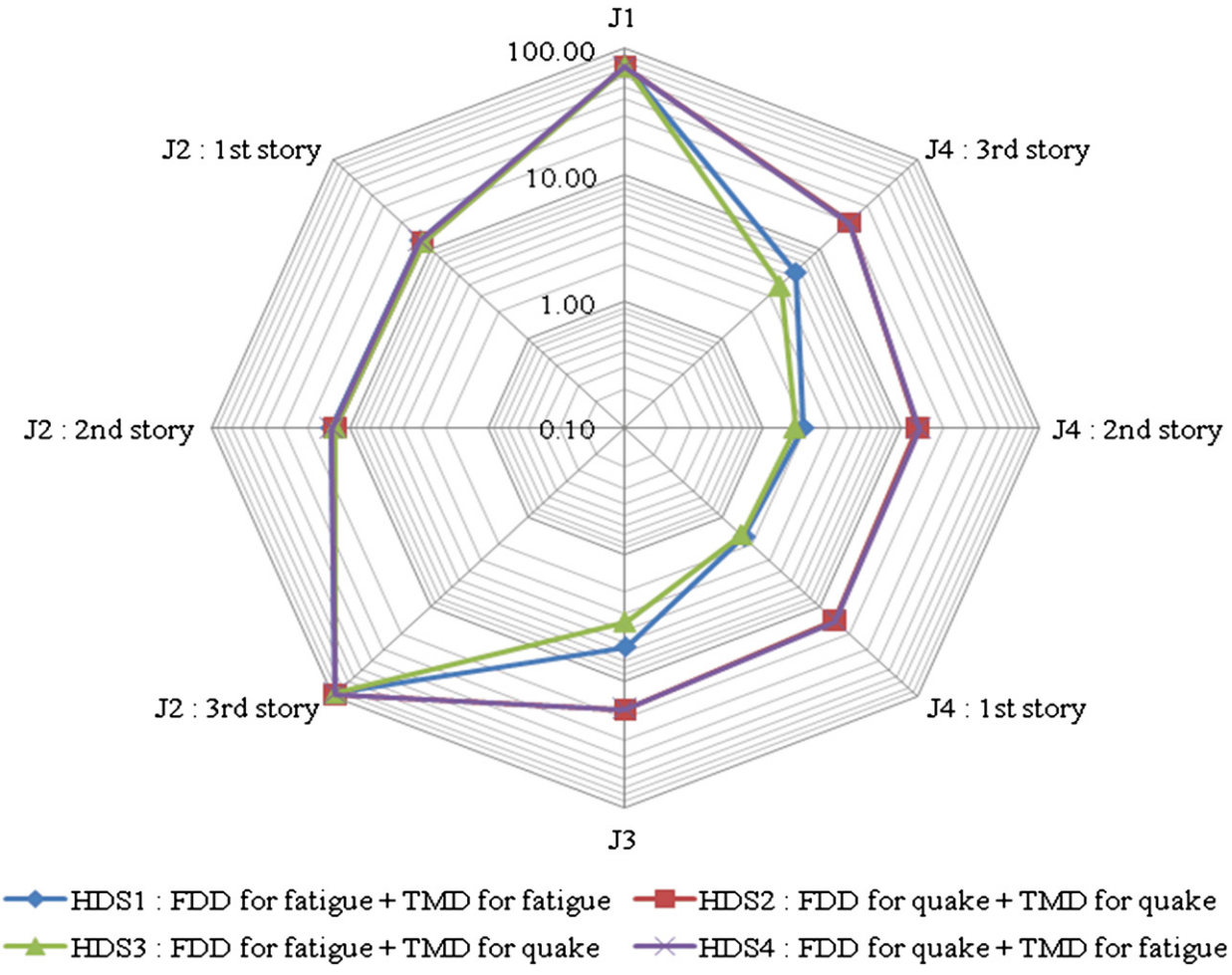

Fig. 7. Performance indices (J_1 to J_4) of HDS variants (log scale), NRB platform.

Table 5
Performance indices of HDS variants (%), FRZ platform.

System	J_1	J_2: 1st story	J_2: 2nd story	J_2: 3rd story	J_3	J_4: 1st story	J_4: 2nd story	J_4: 3rd story
HDS1: FDD for fatigue + TMD for fatigue	24.31	0.36	0.40	80.17	3.34	2.05	2.44	3.58
HDS2: FDD for quake + TMD for quake	26.43	0.33	0.36	85.88	23.98	23.48	20.91	26.83
HDS3: FDD for fatigue + TMD for quake	24.64	0.33	0.36	81.48	5.93	2.20	2.12	3.59
HDS4: FDD for quake + TMD for fatigue	26.41	0.36	0.40	85.52	24.05	23.68	20.89	27.04

2 Numerical simulations confirmed the effectiveness of HDS variants, but showed that the resulted performance is dependent upon how best to make the decision as to which damper should be designed for earthquake and which one for wave-induced fatigue.
3 By combining FDD designed for seismic load and TMD adjusted for wave-induced fatigue or seismic load, the resulted HDS would have the best total performance as compared to other variants of HDS.
4 Effectiveness of HDS in fatigue damage mitigation seems to be much less sensitive to design and adjustment of dampers in comparison with the performance of HDS in seismic vibration control.
5 During this research it was deduced that FDD seems to have much more influence on the effectiveness of HDS rather than TMD. In other words, effectiveness of HDS is mainly dependent upon FDD rather than TMD.
6 Comparison between numerical results for NRB platform and FRZ platform indicates that HDS variants are generally more effective in fatigue damage mitigation for NRB platform which is located in deeper water and has a period larger than that of FRZ platform.
7 In order to mitigate both wave-induced and seismic vibrations of offshore platforms, the possibility of using HDS there exists. However more analyses with more detailed and sophisticated models should be carried out in future works to confirm the effectiveness of HDS.

Several topics requiring further study were identified during the course of this research as listed below.

1 Numerical results and conclusions justify further exploration of the practical feasibility and the cost/benefit comparisons for applications of hybrid damping systems for offshore jacket platforms.
2 Other passive control devices would be examined in order to control both seismic load as well as fatigue damage, e.g. MR dampers, viscous fluid dampers, viscoelastic dampers and so on.

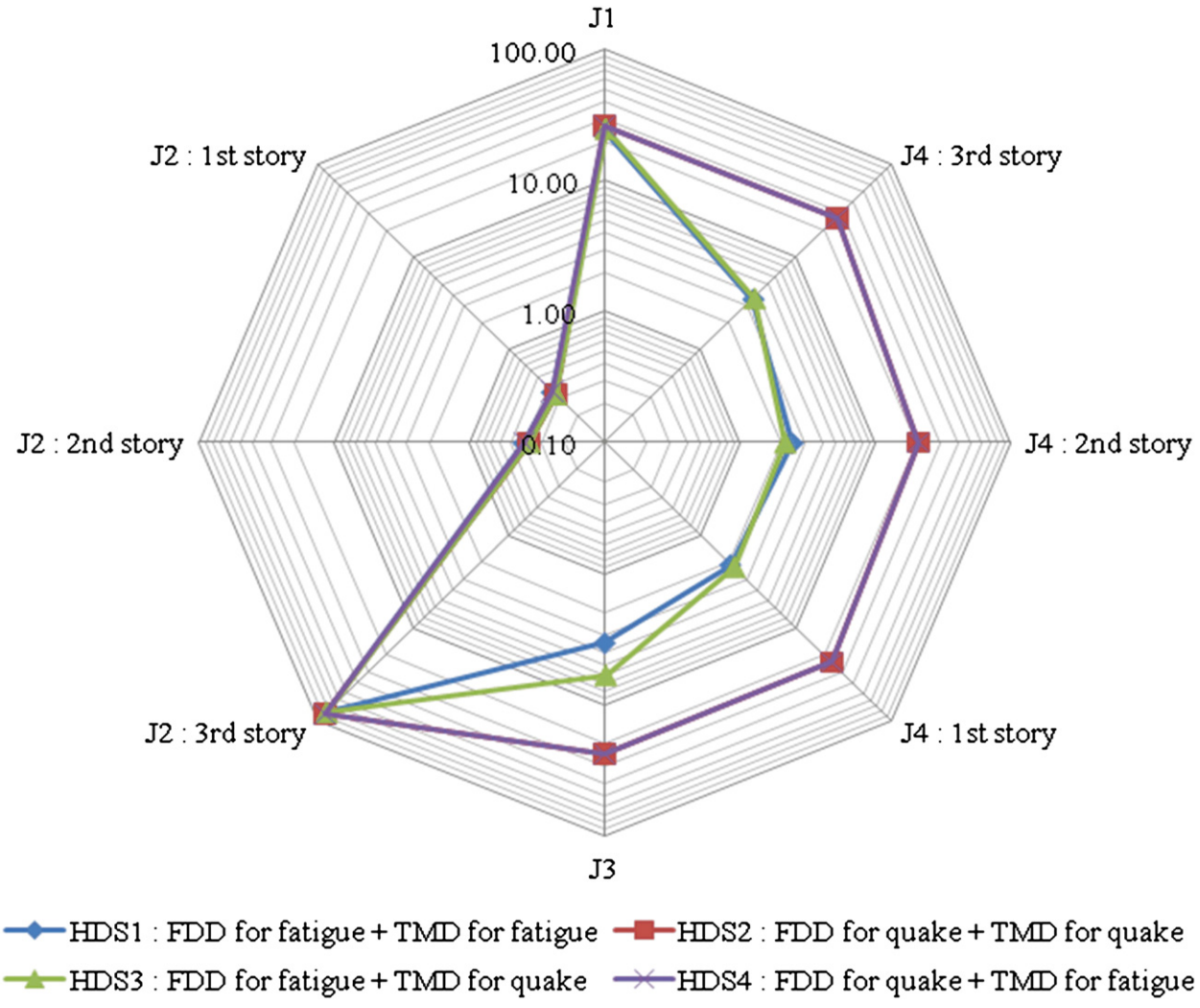

Fig. 8. Performance indices (J_1 to J_4) of HDS variants (log scale), FRZ platform.

3 It is recommended that SSI or SPI to be modeled in future research to examine their effect.
4 In the current study, the criterion for fatigue performance was assumed to be the standard deviation of top displacement and story drifts, but in future research, some other criteria such as stress in critical connections should be investigated.
5 The center-of-damage sea-state was the main focus of this study. However, other sea-states are recommended to be considered in future works.
6 In addition to peak value, it is recommended to use root mean square (RMS) value in order to define seismic performance indices for better comparison in future research.

References

[1] Schoefs F. Sensitivity approach for modelling the environmental loading of marine structures through a matrix response surface. Reliab Eng Syst Saf 2008;93:1004–17.
[2] Ou J, Long X, Li QS, Xiao YQ. Vibration control of steel jacket offshore platform structures with damping isolation systems. Eng Struct 2007;29:1525–38.
[3] Vincenzo G, Roger G. Adaptive control of flow-induced oscillation including vortex effects. Int J NonLinear Mech 1999;34:853–68.
[4] Ou JP, Xiao YQ, Duan ZD, Zou XY, Wu B, Wei JS. Ice-induced vibration control of JZ20-2MUQ platform structure with viscoelastic energy dissipaters. Ocean Eng 2000;18(3):9–14.
[5] Li HJ, Hu SJ, Takayama T. Optimal active control of wave-induced vibration for offshore platforms. China Ocean Eng 2001;15(1):1–14.
[6] Wang S. Semi-active control of wave-induced vibration for offshore platforms by use of MR damper. Proceedings of International Conference on Offshore Mechanics and Arctic Engineering, Oslo, Norway; June 2002. p. 23–8.
[7] Mahadik AS, Jangid RS. Active control of offshore jacket platforms. Int Shipbuilding Prog 2003;50:277–95.
[8] Zhou YJ, Zhao DY. Neural network based active control for offshore platforms. China Ocean Eng 2003;17(3):461–8.
[9] Patil KC, Jangid RS. Passive control of offshore jacket platforms. Ocean Eng 2005;32:1933–49.
[10] Lee HH, Wong SH, Lee RS. Response mitigation on the offshore floating platform system with tuned liquid column damper. Ocean Eng 2006;33:1118–42.
[11] Jin Q, Li X, Sun N, Zhou J, Guan J. Experimental and numerical study on tuned liquid dampers for controlling earthquake response of jacket offshore platform. Mar Struct 2007;20:238–54.
[12] Ma H, Tang GY, Hu W. Feedforward and feedback optimal control with memory for offshore platforms under irregular wave forces. J Sound Vib 2009;328:369–81.
[13] Xu Y, Liu Y, Kan C, Shen Z, Shi Z. Experimental research on fatigue property of steel rubber vibration isolator for offshore jacket platform in cold environment. Ocean Eng 2009;36:588–94.
[14] Yue Q, Zhang L, Zhang W, Kärnä T. Mitigating ice-induced jacket platform vibrations utilizing a TMD system. Cold Reg Sci Technol 2009;56:84–9.
[15] Taflanidis AA, Angelides DC, Scruggs JT. Simulation-based robust design of mass dampers for response mitigation of tension leg platforms. Eng Struct 2009;31:847–57.
[16] Kim DH. Neuro-control of fixed offshore structures under earthquake. Eng Struct 2009;31:517–22.
[17] Golafshani AA, Gholizad A. Friction damper for vibration control in offshore steel jacket platforms. J Constr Steel Res 2009;65(1):180–7.
[18] Golafshani AA, Gholizad A. Passive devices for wave induced vibration control in offshore steel jacket platforms. Sci Iran Transaction A Civ Eng 2009;16(6):443–56.
[19] Gholizad A. Possibility exploration and performance evaluation of vibration control algorithms for offshore platforms. [Ph.D. Dissertation, Supervisor: Ali Akbar Golafshani,] Tehran, Iran: Civil Engineering Department, Sharif University of Technology; 2009 [in Persian].
[20] Kashani M, Golafshani AA, Gholizad A. Vibration control of offshore jacket platforms with hybrid damping systems. Proceedings of 5th World Conference on Structural Control and Monitoring (5WCSCM), Tokyo, Japan; July 2010. p. 12–4.
[21] Golafshani AA, Kashani M, Gholizad A, Dastan MA. Vibration control of offshore platforms by combining dampers. Proceedings of 12th Marine Industries Conference (MIC2010), Zibakenar, Iran; October 19–21 2010 [in Persian].
[22] Gerwick Jr BC. Construction of marine and offshore structures. 2nd ed. CRC Press LLC; 2000.
[23] Mualla IH. Experimental & computational evaluation of a new friction damper device. [Ph.D. Thesis] Department of Structural Engineering and Materials, Technical University of Denmark; 2000.
[24] Mualla IH, Belev B. Performance of steel frames with a new friction damper device under earthquake excitation. Eng Struct 2002;24:365–71.
[25] Soong TT, Dargush GF. Passive energy dissipation systems in structural engineering. New York: John Wiley & Sons; 1997.
[26] Kim JK, Seo YI. Seismic design of steel structures with buckling-restrained knee braces. J Constr Steel Res 2003;59:1477–97.
[27] Kim JK, Choi HH. Displacement-based design of supplemental dampers for seismic retrofit of a framed structure. J Struct Eng 2006;132(6):873–83.
[28] Sadek F, Mohraz B, Taylor AW, Chung RM. A method of estimating the parameters of tuned mass dampers for seismic applications. Earthq Eng Struct Dyn 1997;26:617–35.
[29] Wen YK. Method of random vibration of hysteretic systems. J Eng Mech Div ASCE 1976;102(2):249–63.
[30] Yang JN, Li Z, Liu SC. Stable controllers for instantaneous optimal control. J Eng Mech ASCE 1992;118(8):1612–30.
[31] Chakrabarti SK. Hydrodynamics of offshore structures. Springer-Verlag; 1987.
[32] API RP2A-WSD. Recommended practice for planning, designing and constructing fixed offshore platforms-working stress design. 21th ed. Washington DC: American Petroleum Institute; 2000.
[33] Newland DE. An introduction to random vibrations and spectral analysis. Longman; 1984.
[34] Chakrabarti SK. Hydrodynamics of offshore structures. Computational Mechanics Publications; 1994.
[35] Wilson JF. Dynamics of offshore structures. Hoboken, New Jersey: John Wiley & Sons Inc.; 2003.
[36] Le Mehaute B. An introduction to hydrodynamics and water waves. Water Wave Theories, Volume II, TR ERL 118- POL-3-2, U.S. Washington, DC: Department of Commerce, ESSA; 1969.
[37] Patel MH. Dynamics of offshore structures. Butterworths; 1989.
[38] Yang CY. Random vibration of structures. USA: John Wiley & Sons; 1985.
[39] Chakrabarti SK. Handbook of offshore engineering. Elsevier; 2005.
[40] Dover WD, Mahava Rao AG. Fatigue in offshore structures. Brookfield: Balkema Publishers 2; 1996.
[41] FEMA 356. Prestandard and commentary for the seismic rehabilitation of buildings. Report FEMA 356. Washington DC: Federal Emergency Management Agency; 2000.
[42] PEER NGA database. http://peer.berkeley.edu/smcat . [Accessed on July 2010].
[43] PEER Strong ground Motion Database. http://peer.berkeley.edu/smcat . [Accessed on July 2010].
[44] Kashani M. Analytical studies on vibration control of offshore jacket platforms with hybrid damping systems. [M.Sc. Dissertation, Supervisor: Ali Akbar Golafshani] Tehran, Iran: Civil Engineering Department, Sharif University of Technology; 2010.